sandro and G. Jona-Lasinio, *Adv. Phys.* **27**, 913 (1978)]. The mathematics of self-similar phenomena is elegant, tantalizing, and currently popular [see, for example, recent books on fractal sets and processes, chaotic behavior, and nonlinear dynamical systems, such as G. L. Baker and J. P. Gollub, *Chaotic Dynamics* (Cambridge Univ. Press, Cambridge, 1990); D. Ruelle, *Chance and Chaos* (Princeton Univ. Press, Princeton, NJ, 1991)]. However, attempts at fitting fractal models to various phenomena—such as geologic formations, market fluctuations, cardiac arrhythmias, meteorological anomalies, and fluid turbulence—are tenuous and controversial [see, for example, I. Amato, *Science* **256**, 1763 (1992)].

21. The representation of the total variance of a heterogeneous population that is composed of subpopulations as a sum of within- and between-subpopulation variance is at the core of ANOVA (analysis of variance) methods; see, for example, R. R. Sokal and F. J. Rohlf, *Biometry: The Principles and Practice of Statistics in Biological Research* (Freeman, New York, ed. 2, 1981), pp. 198–205; M. Fisz, *Probability Theory and Mathematical Statistics* (Wiley, New York, ed. 3, 1963), pp. 512–520; C. R. Rao and J. Kleffe, *Estimation of Variance Components and Applications* (Elsevier, New York, 1988).
22. In the simplest case, let the sequence consist of two patch types and assume that any particular window is equally likely to fall into either patch type. The observed variables are then

$$S_{jk}(L) = \sum_{i=k}^{k+L-1} X_j(i)$$

where $X_j(i) = 1$ with probability p_j and -1 with probability $q_j = 1 - p_j$, and $j = 1$ or 2 depending on which patch type the window starting at position k belongs to. The expectation and variance of S_{jk} are $E[S_{jk}] = L(p_j - q_j)$, and $\mathrm{Var}[S_{jk}] = L\,4\,p_jq_j$. Thus, the average within-patch variance is given by $L\,2\,(p_1q_1 + p_2q_2)$, and the between-patch variance is given by

$$\frac{1}{2}L^2[(p_1 - q_1)^2 + (p_2 - q_2)^2] - \frac{L^2}{4}[(p_1 - q_1) + (p_2 - q_2)]^2 = L^2(p_1 - p_2)^2$$

Only in the case $p_1 = p_2$ does the L^2 term vanish.

23. V. V. Prabhu and J.-M. Claverie, *Nature* **359**, 782 (1992).
24. M. Kimura, *The Neutral Theory of Molecular Evolution* (Cambridge Univ. Press, Cambridge, 1983).
25. J. H. Gillespie, *The Causes of Molecular Evolution* (Oxford Univ. Press, Oxford, 1992).
26. S. Karlin and V. Brendel, *Science* **257**, 39 (1992).
27. This work was supported in part by NIH grants HG00335-04 and GM10452-29 and NSF grant DMS86-06244.

16 September 1992; accepted 13 November 1992

The Skipping of Constitutive Exons in Vivo Induced by Nonsense Mutations

Harry C. Dietz,* David Valle, Clair A. Francomano, Raymond J. Kendzior, Jr., Reed E. Pyeritz, Garry R. Cutting

Nonsense mutations create a premature signal for the termination of translation of messenger RNA. Such mutations have been observed to cause a severe reduction in the amount of mutant allele transcript or to generate a peptide truncated at the carboxyl end. Analysis of fibrillin transcript from a patient with Marfan syndrome revealed the skipping of a constitutive exon containing a nonsense mutation. Similar results were observed for two nonsense mutations in the gene encoding ornithine δ-aminotransferase from patients with gyrate atrophy. All genomic DNA sequences flanking these exons that are known to influence RNA splicing were unaltered, which suggests that nonsense mutations can alter splice site selection in vivo.

The fibrillin gene (*FBN1*) encodes a 350-kD glycoprotein component of the extracellular microfibril (*1*). Mutations in this gene cause Marfan syndrome, a systemic disorder of connective tissue with manifestations in the ocular, skeletal, and cardiovascular systems (*2–4*). Although the genomic organization of the gene has not been determined, approximately 7 of 10 kb of *FBN1* cDNA have been cloned and sequenced (*5*). The characterization of *FBN1* defects that cause Marfan syndrome resulted in the identification in one patient of an allele with a 66-nucleotide (nt) deletion in mature mRNA resulting from in-frame skipping of an entire exon. This patient had no family history of Marfan syndrome but had classic and severe manifestations of the disorder. The only identified sequence variation unique to this patient was a T → G transversion at position +26 of the skipped exon, which resulted in a premature TAG termination codon. Exon skipping restored the open reading frame of the mutant transcript. Alternative splicing was not observed in either parent of the patient or in 70 unrelated individuals. We subsequently observed two recurrences of this phenomenon in patients with different nonsense mutations in the gene (*OAT*) for ornithine δ-aminotransferase (OAT), a nuclear-encoded mitochondrial matrix enzyme. Mutations in *OAT* cause gyrate atrophy (GA), an autosomal recessive, slowly progressive chorioretinal degeneration leading to blindness in middle age. We propose that these nonsense mutations induce the skipping of constitutive exons in vivo.

A 540-nt fragment of *FBN1* cDNA was amplified by the polymerase chain reaction (PCR) and subjected to single-strand conformation polymorphism analysis. An abnormally migrating band unique to a sample from a patient with classic Marfan syndrome (patient MS-7) was observed (*6*). Reamplification of DNA recovered from the abnormal band showed a heteroduplex that contained a wild-type product (540 bp) and a smaller (474 bp) product. Direct sequencing of each template demonstrated a 66-bp deletion in the smaller product (Fig. 1) that encompassed the 3′ region of one of five eight-cysteine domains in *FBN1* that are homologous to a motif found in transforming growth factor–β1 binding protein (*5*). This cysteine-rich domain may participate in protein-to-protein interactions.

The sequencing of PCR-amplified genomic DNA revealed that the deleted 66-bp region of cDNA represents an entire exon (hereafter referred to as exon B) (Fig. 2A). To determine the basis for exon skipping, we amplified by PCR a 3.0-kb region of genomic DNA from MS-7, his parents, and an unrelated and unaffected individual (Co1). The resulting product spanned the 3′ end of the upstream exon (A), the skipped exon (B), and two downstream exons (C and D). With the exception of the central 2.0 kb of the intron following exon C (intron C), this region was sequenced for all four individuals (Fig. 2B). A wild-type sequence was observed for all of the cis-acting elements known to influence RNA splicing, including the 3′ and 5′ splice sites and the predicted branchpoint flanking exon B (*7–9*) in all samples. Patient MS-7's sample, however, had a unique mutation: a T → G substitution in one allele at position +26 in exon B (Fig. 2C). The corresponding amino acid alteration is a substitution of a termination codon (X) for tyrosine (Y) at codon 1215 (Y1215X) in the characterized coding sequence for *FBN1* (*5*). A Cvn I restriction site is created by this alteration and can be used to screen DNA for mutation Y1215X (*6*). None of 55 unaffected control subjects and 52 unrelated probands with Marfan syndrome carried this defect.

Another single base substitution was identified at position −64 of intron A. Patient MS-7 was heterozygous A/G, his mother was A/A, his father was G/G, and Col was A/G. This polymorphism occurs away from the conventional placement for a branchpoint sequence (positions −18 to −40) and within a context without homol-

H. C. Dietz, C. A. Francomano, R. J. Kendzior, Jr., R. E. Pyeritz, G. R. Cutting, Departments of Pediatrics and Medicine, The Johns Hopkins University School of Medicine, Baltimore, MD 21205.
D. Valle, Howard Hughes Medical Institute, Department of Pediatrics, The Johns Hopkins University School of Medicine, Baltimore, MD 21205.
*To whom correspondence should be addressed.

ogy to the branchpoint consensus (*10, 11*).

To determine if the polymorphism in intron A influences precursor mRNA (pre-mRNA) splicing in fibroblasts or whether alternative splicing of exon B normally occurs, we reverse-transcribed total fibroblast RNA and a PCR-amplified DNA fragment that spanned the region of exon B from MS-7, his parents, Co1, 55 unrelated probands with Marfan syndrome, and 15 unrelated and unaffected individuals. A product of the size predicted by the skipping of exon B was unique to MS-7's sample (Fig. 3). The amount of cDNA amplified from the mutant allele was approximately 25% of the amount observed from the wild-type allele [quantification was performed by standard procedures (*12*)]. Cvn I digestion of PCR-amplified total fibroblast cDNA from MS-7 indicated undetectable amounts of transcript that contained the premature termination codon (6).

To assess whether the ability of nonsense mutations to induce exon skipping was context-specific, we studied the transcript of two gyrate atrophy patients with different nonsense mutations in constitutive exons of the gene encoding OAT (*13*). Patient GA035 is homozygous for a G → A transition at position +13 of exon 6 (W178X, 128-bp exon, where W is Trp and X is a termination codon), whereas patient GA003 is heterozygous for a G → A transition at position +53 of exon 8 (W275X, 129-bp exon) (*14*). When fibroblast total RNA was reverse-transcribed and amplified with primers with an OAT gene–specific sequence from exons 5 and 9, a normal-size product (534 bp) and a shortened product (~400 bp) were observed for each patient. Only the larger product was amplified from unaffected individuals. Direct sequencing of the smaller fragments of DNA revealed selective skipping of exon 6 in the transcript from patient GA035 and the skipping of exon 8 in the transcript from patient GA003 (Fig. 4). In both cases, the amount of cDNA amplified from the abnormally spliced transcript was less than 5% of that amplified from the transcript of normal size (*12*).

Sequences within an exon can influence splice site selection (*15–19*). The first two and last three nucleotides of the exon con-

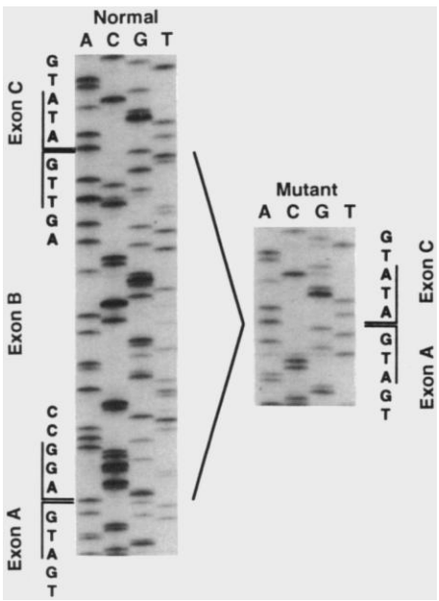

Fig. 1. Sequence of *FBN1* cDNA from the normal and mutant alleles of patient MS-7. The mutant sequence reveals a 66-bp deletion extending from nt 3620 to 3685 [nucleotide and codon numbering as in (*5*)]. Reverse transcription–PCR of fibroblast total RNA was performed as described (*3*) with primers F11S and F11AS [oligonucleotide sequences as in (*27*)]. After single-strand conformation polymorphism analysis (*28*), DNA from an abnormal heteroduplex band was eluted from the gel and used as template for PCR amplification with primers F11S and F11AS. Two products were produced, one of the expected size (540 bp) and one smaller (474 bp). These products were purified by gel electrophoresis and sequenced with primer F11BAS and a cycle sequencing kit (Bethesda Research Laboratories). Although sequencing was performed with an antisense primer, the result is displayed in the sense orientation for ease of reading.

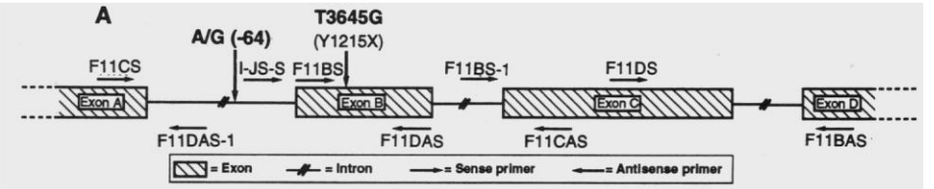

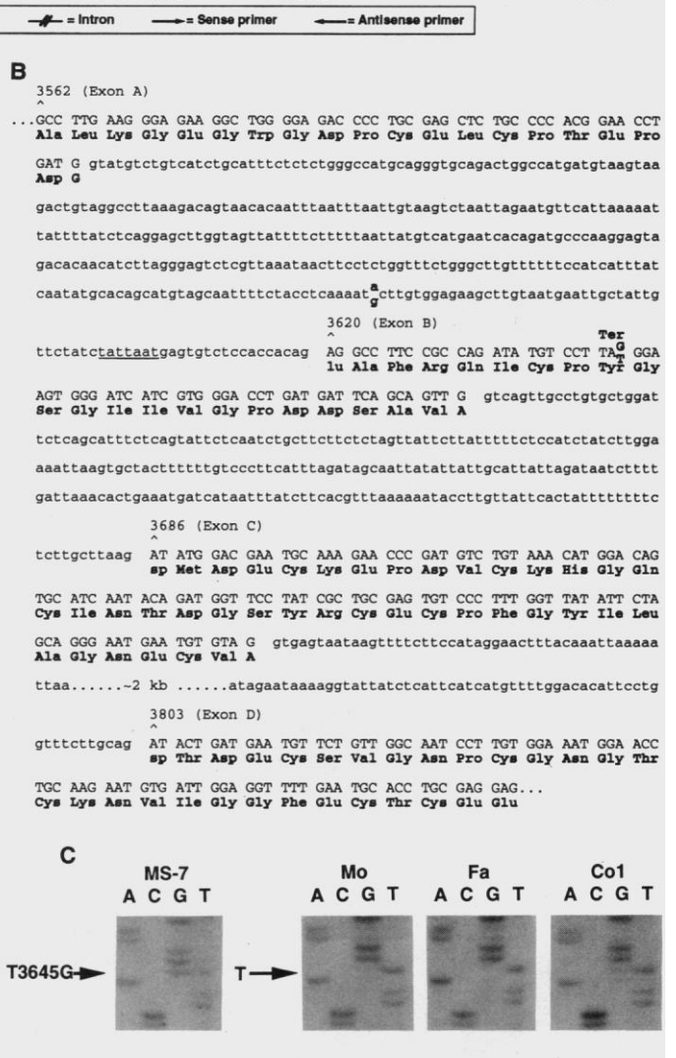

Fig. 2. *FBN1* genomic DNA sequence in the region of exon B and variations in patient MS-7, his mother (Mo), father (Fa), and a control subject (Co1). (**A**) Schematic representation of a genomic DNA fragment amplified by PCR (*29*) with primers F11CS and F11BAS that spans the 3′ end of exon A, exon B, and exon C and the 5′ end of exon D. (**B**) Sequence of the genomic DNA fragment illustrated in (A). Sequencing was performed as described (*2, 3*). Exon and intron DNA sequences are shown in uppercase and lowercase letters, respectively. Boldfaced nucleotides represent points of sequence variation. The deduced amino acid sequence is written below the corresponding codons. The 5′ nucleotides in exons B, C, and D are numbered according to their position in the partial fibrillin cDNA sequence (*5*). The 5′ base shown for exon A and the complement of the 3′ base shown for exon D correspond to the 5′ nucleotides of the primers used to amplify this fragment. The underlined sequence best fits the branchpoint consensus YNYURAY, where Y = pyrimidine, N = any nucleotide, U = uridine, R = purine, and A = branchpoint A residue (*9*). (**C**) Sequence of exon B from MS-7, his parents, and Co1 showing the G → T transversion at nt 3645 unique to one allele of MS-7. PCR-amplified genomic DNA was sequenced with primer I-JS-S.

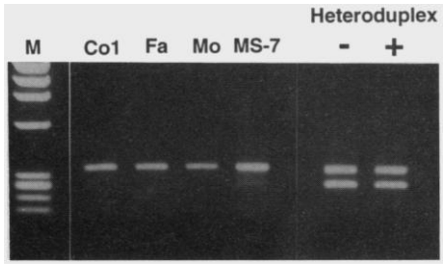

Fig. 3. Reverse transcription–PCR analysis of *FBN1* transcript spanning the region of exon B from MS-7, his parents (Mo and Fa as in Fig. 2), and Co1. PCR amplification was performed with primers F11CS and F11BAS. Upper (wild-type) band is 327 bp. The lower (261 bp) fragment is unique to MS-7's samples and shows the skipping of exon B. Total fibroblast cDNA or DNA recovered from the single-strand conformation polymorphism analysis heteroduplex band from patient MS-7 served as template. The heteroduplex-derived product was either undigested (−) or digested with Cvn I (+). The lack of any apparent digestion of either band in the heteroduplex (+) lane demonstrates undetectable amounts of transcript containing the premature termination codon. The same result was observed upon digestion of PCR-amplified total fibroblast cDNA from patient MS-7 (*6*). M, Hae III–digested ΦX DNA.

tribute to the recognition of 3′ and 5′ splice sites, respectively (*20, 21*). Less is understood about the role of internal exon sequences in the splicing mechanism. Experimental creation of large insertions, deletions, or multiple nucleotide substitutions within exons that normally display regulated alternative splicing can influence splice site selection by altering the optimal distance between the 3′ and 5′ splice junctions, inactivating cis-acting elements, or creating unfavorable secondary structure within the exon (*11, 15, 17*). The skipping of a constitutive exon has been demonstrated in response to both an intraexonic deletion and a missense mutation that activates a cryptic splice site (*18, 19*). Alteration in factor binding or RNA secondary structure has been proposed as the basis for these observations.

Whether the skipping of exons that contain nonsense mutations is a consequence of altered RNA secondary structure or the creation of a premature termination codon is unknown. The latter hypothesis is strengthened by our inability to detect any abnormally spliced transcript in patients with missense mutations or polymorphisms in *FBN1* (*2–4*) and by multiple examples of regulated expression of exons that contain constitutive stop codons. Such exons undergo tissue-specific splicing in the human *N-CAM* gene, developmental stage-specific splicing in the rat glutamic acid decarboxylase gene, and sex-specific splicing in the *sex lethal* (*sxl*) gene of *Drosophila melanogaster* (*22–24*). The recognition of nonsense codons before RNA splicing requires a mechanism to read pre-mRNA exon sequences in-frame by either direct coupling between translation and RNA processing or a scanning function by ribosomelike molecules in the nucleus (*25*).

Gyrate atrophy is an autosomal recessive disorder that results from a deficiency of enzymatically active OAT. It is unlikely that the abnormally spliced transcript observed in patients GA035 and GA003 produces any functional protein or that abnormal splicing of *OAT* influences the phenotype of these patients. In contrast, *FBN1* encodes a structural protein, the amount of abnormally spliced transcript is relatively high, and a dominant negative mechanism has been proposed for Marfan syndrome (*3*). In this light, the predicted product of patient MS-7's abnormally spliced *FBN1* transcript, missing a central domain encoded by a single exon, may indeed have a pathogenic role.

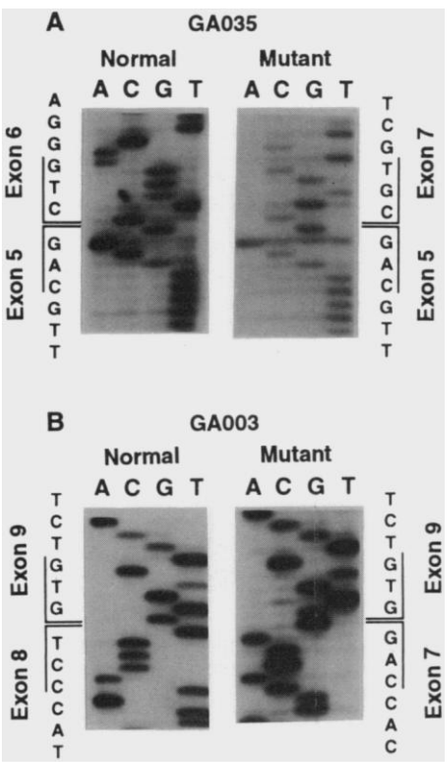

Fig. 4. Direct sequencing of reverse-transcribed and amplified *OAT* transcript from patients (**A**) GA035 and (**B**) GA003 with nonsense mutations in exons 6 and 8, respectively. PCR (spanning exons 5 to 9) and sequencing were performed with primers OATE5-S and OATE9-AS. Sequences for both the normal-size (normal) and shortened (mutant) products are shown for each patient. Although sequencing of samples from GA003 was performed with an antisense primer, the results are displayed in the sense orientation for ease of reading.

Note added in proof: It has been recently demonstrated that nonsense mutations introduced into open reading frames of the autonomous parvovirus minute virus of mice (MVM) act in cis to alter the usage of alternatively spliced sequences in viral RNA in the nuclei of murine cells (*26*).

REFERENCES AND NOTES

1. L. Y. Sakai, D. R. Keene, E. Engvall, *J. Cell Biol.* **103**, 2499 (1986).
2. H. C. Dietz *et al.*, *Nature* **352**, 337 (1991).
3. H. C. Dietz *et al.*, *J. Clin. Invest.* **89**, 1674 (1992).
4. H. C. Dietz *et al.*, *Hum. Mutat.*, in press.
5. C. L. Maslen *et al.*, *Nature* **352**, 334 (1991).
6. H. C. Dietz *et al.*, data not shown.
7. R. A. Padgett *et al.*, *Annu. Rev. Biochem.* **55**, 1119 (1986).
8. T. Maniatis and R. Reed, *Nature* **325**, 673 (1987).
9. P. A. Sharp, *Science* **235**, 766 (1987).
10. B. Ruskin *et al.*, *Cell* **38**, 317 (1984).
11. M. B. Somasekhar and J. E. Mertz, *Nucleic Acids Res.* **13**, 5591 (1985).
12. Patient fibroblast total RNA was isolated from three separate cultures. Reverse-transcribed cDNA was amplified with primers F10BS and F11CAS. The product was electrophoresed, transferred to a Southern (DNA) blot, and hybridized to radiolabeled oligonucleotide F11S by standard methods (*3*). Filter fragments that corresponded to the positions of the normally and aberrantly spliced products on an autoradiograph were excised, and the signal was counted with a scintillation counter (Beckman LS 1801). The signal from the abnormally spliced product ranged from 20 to 29% of that from the wild-type product. Abnormally spliced *OAT* transcript was quantified with identical methods. Reverse-transcribed cDNA was amplified with primers OATE5-S and OATE9-AS. The Southern blot–transferred product was hybridized to radiolabeled oligonucleotide OATE7-S (exon 7–specific sequence).
13. G. A. Mitchell *et al.*, *J. Biol. Chem.* **263**, 14288 (1988).
14. D. Valle, unpublished data.
15. R. Reed and T. Maniatis, *Cell* **46**, 681 (1986).
16. M. H. Ricketts *et al.*, *Proc. Natl. Acad. Sci. U.S.A.* **84**, 3181 (1987).
17. H. J. Mardon, G. Sebastio, F. E. Baralle, *Nucleic Acids Res.* **15**, 7725 (1987); R. K. Hampson, L. LaFollette, F. M. Rottman, *Mol. Cell. Biol.* **9**, 1604 (1989); A. Y. M. Tsai, M. Streuli, H. Saito, *ibid.*, p. 4550; D. Libri, M. Goux-Pelletan, E. Brody, M. Y. Fiszman, *ibid.* **10**, 5036 (1990); A. C. Chain, S. Zollman, J. C. Tseng, F. A. Laski, *ibid.* **11**, 1538 (1991); L. Domenjoud, H. Gallinaro, L. Kister, S. Meyer, M. Jacob, *ibid.*, p. 4581; T. A. Cooper, *J. Biol. Chem.* **267**, 5330 (1992).
18. M. Matsuo *et al.*, *J. Clin. Invest.* **87**, 2127 (1991).
19. N. Wakamatsu, H. Kobayashi, T. Miyatake, S. Tsuji, *J. Biol. Chem.* **267**, 2406 (1992).
20. S. M. Mount, *Nucleic Acids Res.* **10**, 459 (1982).
21. Y. Oshima and Y. Gotoh, *J. Mol. Biol.* **195**, 247 (1987).
22. H. J. Gower *et al.*, *Cell* **55**, 955 (1988).
23. R. W. Bond, R. J. Wyborski, D. I. Gottlieb, *Proc. Natl. Acad. Sci. U.S.A.* **87**, 8771 (1990).
24. L. R. Bell *et al.*, *Cell* **55**, 1037 (1988).
25. G. Urlaub, P. J. Mitchell, C. J. Ciudad, L. A. Chasin, *Mol. Cell. Biol.* **9**, 2868 (1989).
26. L. K. Naeger, R. V. Schoborg, Q. Zhao, G. E. Tullis, D. J. Pintel, *Genes Dev.* **6**, 1107 (1992).
27. The sequences for oligonucleotides used in this study are as follows. *FBN1*: F11S (5′-TGAGCTACTGTTATGCGAAG-3′; nt 3479 through 3498), F11AS (5′-GCACATATCCCACGGGAC; nt 4018 through 4001), F11BAS (5′-CTCCTCGCAGGTGCATTC-3′; nt 3888 through 3871), F11CS (5′-

GCCTTGAAGGGAGAAGGC-3'; nt 3562 through 3579), I-JS-S (5'-GAGAAGCTTGTAATGAATTGC-3'; nt −57 to −37 from the 5' base of exon B), F11CAS (5'-CAGACATCGGGTTCTTTGC-3'; nt 3716 through 3698), and F10BS (5'-TCCAGAAGGGTTTTCCTTG-3'; nt 3426 through 3444); the numbering of nucleotides is as in (*4*). *OAT*: OATE5-S (5'-GAGACTGCCTGTAAACTAGC-3'; nt 439 through 458), OATE9-AS (5'-ACCGTATGTGGACCCATGC-3'; nt 972 through 954), and OATE7-S (5'-GAGAGCTCTGCACCAGGCAC-3'; nt 748 through 767); the numbering is as in (*13*).

28. J. Michaud *et al.*, *Genomics* **13**, 389 (1992).
29. PCR amplification of genomic DNA with primers F11CS and F11BAS was performed as described (*3*), except that denaturing, annealing, and extension times were extended to 1 min, 1.5 min, and 3 min, respectively.
30. We thank H. H. Kazazian, Jr., and A. F. Scott for critical review of the manuscript. Supported in part by NIH grants AR-41135, HG-00373, RR-00722, DK-44003, and HL-02815, the National Marfan Foundation, and an institutional research grant from the Johns Hopkins University School of Medicine. H.C.D. is a Ross Research Scholar. G.R.C. is a Merck Clinician Scientist.

2 July 1992; accepted 5 November 1992

The Effect of Posttranslational Modifications on the Interaction of Ras2 with Adenylyl Cyclase

Yuichi Kuroda, Noboru Suzuki, Tohru Kataoka*

Ras proteins undergo a series of posttranslational modifications that are critical for their cellular function. These modifications are necessary to anchor Ras proteins to the membrane. Yeast Ras2 proteins were purified with various degrees of modification and examined for their ability to activate their effector, adenylyl cyclase. The farnesylated intermediate form of Ras2 had more than 100 times higher affinity for adenylyl cyclase than for the unprocessed form. The subsequent palmitoylation reaction had little effect. In contrast, palmitoylation was required for efficient membrane localization of the Ras2 protein. These results indicate the importance of farnesylation in the interaction of Ras2 with its effector.

The yeast *Saccharomyces cerevisiae* has two *RAS* genes, which encode proteins that are structurally, functionally, and biochemically similar to mammalian Ras oncoproteins (*1, 2*). The yeast Ras proteins are essential, positive controlling elements of adenylyl cyclase (*3, 4*). Yeast cells possessing the activated *RAS2* gene display abnormal phenotypes, including sensitivity to heat shock, sensitivity to nutritional starvation, and failure to sporulate (*3, 5*). Mammalian Ras proteins can substitute for yeast Ras proteins and activate yeast adenylyl cyclase (*2, 4*).

The Ras2 protein undergoes a series of posttranslational modifications (*6, 7*) that are common to members of the Ras protein family (*8*). The first stage of the processing consists of three modifications of a CAAX motif (C, cysteine; A, aliphatic; and X, any amino acid) at the COOH-terminus: (i) farnesylation of the cysteine residue (Cys^{319}); (ii) proteolytic cleavage of the amino acids AAX; and (iii) methyl-esterification of the new COOH-terminal cysteine. This first stage of processing converts the primary translation product into an intermediate form. The second posttranslational modification of Ras2 is acylation with palmitic acid on a cysteine residue (Cys^{318}) upstream of the CAAX motif. The first stage of processing is a prerequisite for the second stage.

Department of Physiology, Kobe University School of Medicine, 7-5-1 Kusunoki-cho, Chuo-ku, Kobe 650, Japan.

*To whom correspondence should be addressed.

These modifications are essential for the anchoring of mammalian Ras proteins to the cytoplasmic membrane (*9, 10*) and for the transformation of NIH 3T3 cells (*9, 10*), induction of neuronal differentiation of PC12 cells (*11*), and induction of germinal vesicle breakdown in *Xenopus laevis* oocytes (*12*) by activated Ras. However, in vertebrate systems, the effect of the modifications on the activity of Ras proteins could not be examined separately from their effects on membrane anchoring. In budding yeast, an in vitro system exists for studying the interaction of Ras proteins with an effector. It has been shown that the unprocessed Ras2 protein from yeast produced in *Escherichia coli* can activate yeast adenylyl cyclase (*4, 13*). Thus, posttranslational modifications are not absolutely required for the interaction of Ras2 with its effector.

We purified various modified forms of Ras2 and observed their differential action on yeast adenylyl cyclase. The wild-type *RAS2* gene was cloned into a baculovirus transfer vector and overexpressed in Sf9 insect cells (*14*). Fully processed (mature) Ras2 was purified from a detergent extract of the insect cells (*15*). To purify the intermediate and the unprocessed forms of Ras2 proteins, we constructed *RAS2* genes with serine in place of Cys^{318} or Cys^{319} by site-specific mutagenesis and used these genes for overproduction of mutant Ras2 in insect cells (*16*). The three forms of Ras2 protein were purified almost to homogeneity and had apparent molecular sizes of 41 kD (unprocessed form) and 40 kD (intermediate and mature forms) (Fig. 1A). The three forms were characterized by incorporation of ^{3}H-labeled palmitic acid and by C4 reversed-phase chromatography (*6*) (Fig. 1). The incorporation of palmitic acid was observed only in the putative mature form. The elution positions of the three, purified forms of Ras2 in C4 reversed-phase chromatography and their apparent molecular sizes were identical to those reported for the respective forms produced in yeast cells (*6*). No difference was observed in the rate of guanosine triphosphate (GTP) binding and in the affinities for both GTP and guanosine diphosphate (GDP) among the three forms (*17*).

We next examined the ability of the three forms of Ras2 to activate yeast adenylyl cyclase. A crude membrane fraction of yeast cells harboring a plasmid that overexpresses the yeast adenylyl cyclase gene (*CYR1*) was assayed for adenylyl cyclase activity in the presence of Mg^{2+}, guanosine-5'-*O*-(3-thiotriphosphate) (GTP-γ-S), and various concentrations of each of the purified forms of Ras2 (*18*) (Fig. 2, A and C). Both the mature and the intermediate forms were 100 times more potent at activating adenylyl cyclase than the unprocessed form. The maximal extent of the activation caused by each of the three forms was similar. The activation by the unprocessed form was comparable to that obtained with Ras2 protein produced in *E. coli* (*4, 13, 19*). We assumed that the extent of activation reflected association with Ras2 protein and calculated the apparent dissociation constants (K_d's) from Scatchard plots to be about 3, 4, and 400 nM for the mature, intermediate, and the unprocessed forms, respectively.

To determine whether the observed differential action of the three forms resulted from enhanced association with adenylyl cyclase or with the cell membranes, we conducted a similar assay with adenylyl cyclase that was solubilized by extraction with 1.3 M NaCl (*20*) (Fig. 2, B and C). The soluble adenylyl cyclase was activated by the mature and the intermediate forms at concentrations similar to those that activated the membrane-bound adenylyl cyclase; the apparent K_d values were 3 nM for both of them. The unprocessed form was less effective. The apparent K_d was 1.6 μM, but the maximal extent of activation was comparable to that caused by the processed forms. Thus, the differential actions of the three forms do not appear to be explained by a difference in their ability to bind to membranes. The observed 100-fold increase in the apparent affinity for adenylyl cyclase resulted from the first stage of posttranslational processing, presumably the farnesylation of Ras2 protein. The subse-